

Electronic Supplementary Information for:

Thermal Reorganization of Alkyl-substituted Thienothiophene Semiconductors

Vladimir A. Pozdin,[†] Detlef-M. Smilgies,^{‡,*} Hon Hang Fong,^{†,§} Michael L. Sorensen,[¶] and Mingqian He^{¶,*}

[†]Department of Materials Science and Engineering, Cornell University, Ithaca, NY 14853

[‡]Cornell High Energy Synchrotron Source, Cornell University, Ithaca, NY 14853

[§]Department of Electronic Engineering, Shanghai Jiao Tong University, Shanghai 200240, China

[¶]Corning, Inc., SP-FR-6, Corning, NY 14830

*to whom correspondence should be addressed; E-mail: dms79@cornell.edu; hem@corning.com

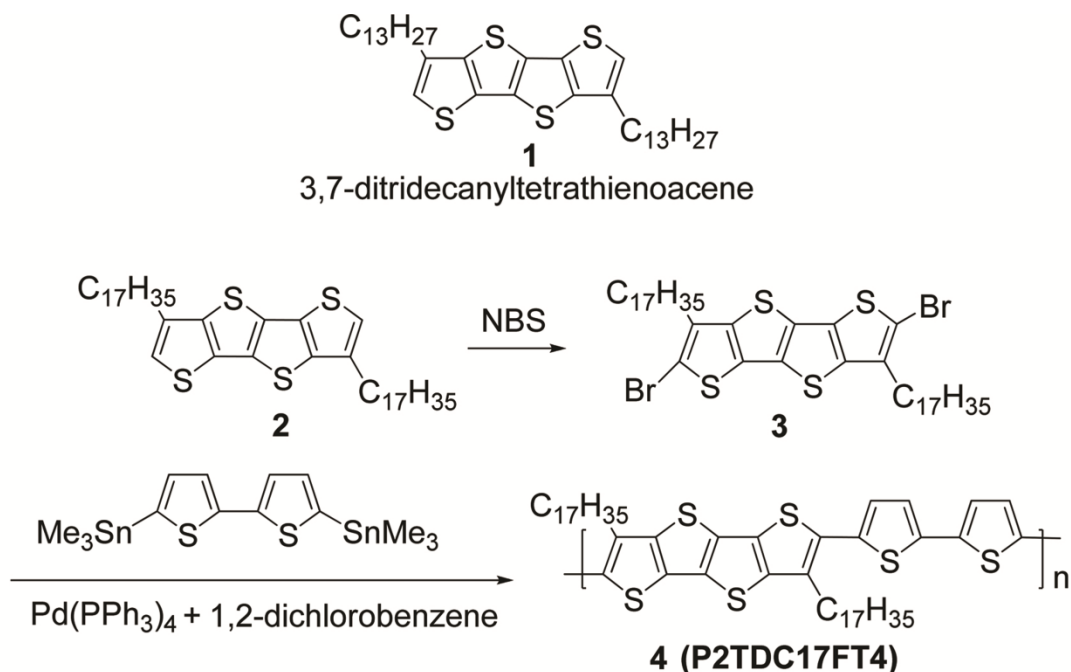
Synthesis

Poly(2,5-bis(thiophene-2-yl)-(3,7 dihepta-decanyltetrathienoacene) (P2TDC17FT4) was synthesized using the following procedures (Scheme S1). Compounds **1** (3,7-ditridecanyltetrathienoacene) and **2** (3,7-dihepta-decanyltetrathienoacene) were synthesized according to our previous methods.¹

2,6-dibromo-3,7- dihepta-decanyltetrathienoacene (3). A dry, 50-mL, three-necked, round bottomed flask fitted with nitrogen inlet was charged with 15 mL of dichloromethane (CH₂Cl₂) and 1.00 g (1.37 mmol) of 3,7-dihepta-decanyltetrathienoacene (**2**). To the stirred suspension a solution of 0.71 g (4.00 mmol) of NBS in DMF (3 mL) was added dropwise. The resulting mixture was stirred at room temperature for 24 hours until TLC indicated no 3,7-dihepta-decanyltetrathienoacene was left and only 2,6-dibromo-3,7- dihepta-decanyltetrathienoacene (**3**) was formed. The reaction was quenched with the addition of sat. Na₂S₂O₃ (10 mL). Evaporation of the solvent gave the crude 2,6-dibromo-3,7-diheptadecanyltetrathienoacene which was washed by water (10 mL x 2) and methanol (10 mL). Recrystallization from toluene (15 mL) afforded 1.1 g (90% yield) of 2,6-dibromo-3,7- dihepta-decanyltetrathienoacene (**3**) as an off-white solid. Mp 135.5-136.5°C; R_f 0.77 (Hexanes); ¹H NMR (300 MHz, CD₂Cl₂, 75 °C): δ 2.76 (4 H, t), 1.74 (4 H, m), 1.38-1.26 (56 H, m), 0.88 (6 H, t).

Poly(2,5-bis(thiophene-2-yl)-(3,7- dihepta-decanyltetrathienoacene) (4). 2,6-dibromo-3,7-diheptadecanyltetrathienoacene (**3**) (0.50 g, 0.56 mmol) and 1,1'-[2,2'-bithiophene]-5,5'-diylbis[1,1,1-trimethylstannane] (0.28 g, 0.56 mmol) were dissolved into chlorobenzene (30 mL) in a flask. Nitrogen was bubbled through this flask for a few minutes. Tetrakis(triphenylphosphine)palladium(0) (0.032 g, 0.0277 mmol) was added to this mixture. This flask was heated to 150-160°C under nitrogen overnight

before being poured into methanol (400 mL) and concentrated hydrochloric acid (20 mL) solution and stirred overnight at room temperature. The precipitate was filtered and extracted in a Soxhlet with acetone and hexane 24 h each. The obtained polymer was then dissolved into chlorobenzene and filtered and precipitated in methanol. The collected polymer **4** was dried in vacuum to yield 0.44 grams (88 %). ^1H NMR (300 MHz, CD_2Cl_2): δ 7.28-6.75 (br m, 4 H), 3.14-2.69 (br m, 4 H), 1.83 (br p, 4 H), 1.53-0.95 (m, 56 H), 0.92 (br s, 6 H).



Scheme S1 Structure of compound **1** and synthetic scheme for compound **4** (P2TDC17FT4).

Vacuum Annealing

Reorganization in the thin film upon thermal annealing is frequently attributed to the removal of residual solvent from a spun cast film. Such is not the case in the polythienothiophene system studied here, as we observe a unit cell expansion upon annealing rather than a contraction, which would be expected to occur, if excess solvent molecules were removed from the unit cell. In order to further rule out the possibility of solvent effects, we utilized vacuum annealing. High vacuum (10^{-6} Torr) causes boiling point depreciation, with the boiling point of common solvents dropping to below room temperature. Thus the excess solvent is driven out without adding energy to the system, which could otherwise drive conformational changes.

Thin films of P2TDC13FT4 were spun cast on silicon wafers with a 200 nm thermally grown silicon dioxide layer. The substrates were cleaned by sonication in semiconductor grade acetone and isopropyl alcohol for 10 min in each solvent, then given a 15 min UV ozone plasma treatment. Solutions of polymers in 1,2-dichlorobenzene (3 mg/mL) were prepared by heating to 170°C for 30 min with stirring to speed up dissolution. Polymer films were then deposited by spin casting at 1000 rpm for 60 s. The structure of the polymer films was analyzed using X-ray diffraction (XRD) with a Scintag diffractometer, employing a Cu target ($\lambda=1.5405 \text{ \AA}$). A θ - 2θ scan with a step size of 0.02° was set up between 4° and 7° to probe the first-order lamellar diffraction peak. Thin film samples were vacuum annealed in a custom deposition chamber with vacuum pressure reaching $<10^{-6}$ Torr. A custom-built substrate heating stage was used to thermally anneal some of the samples that were under vacuum.

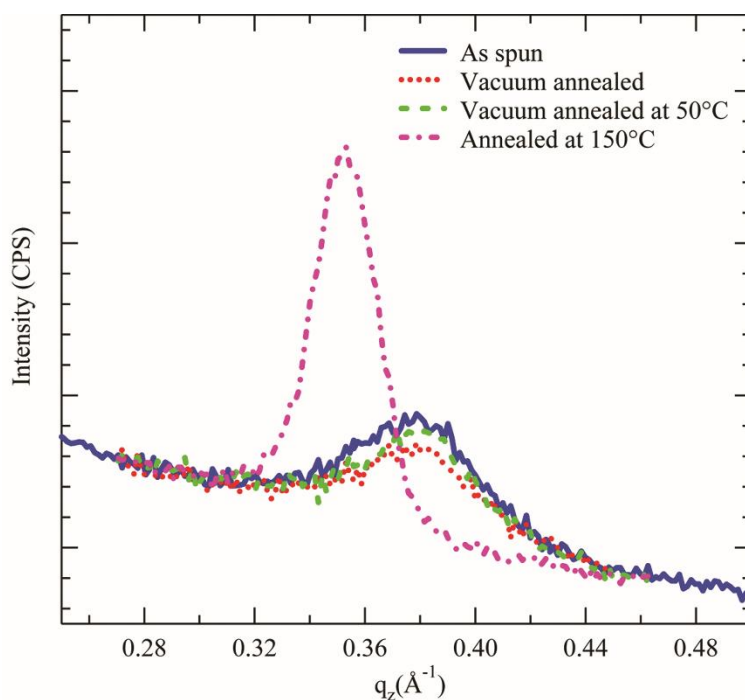


Fig. S1 XRD patterns of the P2TDC13FT4 polymer film cast on SiO_2 surface as spun, after 13 hours of vacuum annealing, after 13 hours of vacuum annealing at 50°C , and after 10 minutes of annealing at 150°C in nitrogen atmosphere.

The results of vacuum annealing experiments are shown in Fig. S1. Spun cast samples with no vacuum or thermal annealing had lamellar spacing of 16.5 \AA . After vacuum annealing for 13 hours, no change in the lamellar spacing was observed. Further vacuum annealing with samples heated to 50°C for another 13 hours to ensure that no solvent remained, caused no changes in the lamellar spacing. However, once the sample was annealed in nitrogen filled glove box at 150°C for 10 minutes, the lamellar spacing

increased to 17.9 Å. The lack of changes in lamellar spacing during vacuum annealing, even at slightly elevated temperatures, rules out the possibility of residual solvent causing the lamellar reorganization upon thermal annealing for P2TDC13FT4. In addition, we observed a significant reduction in the peak width at half maximum upon thermal annealing at 150°C, indicating improved ordering.

Side-Chain Tilt Calculations

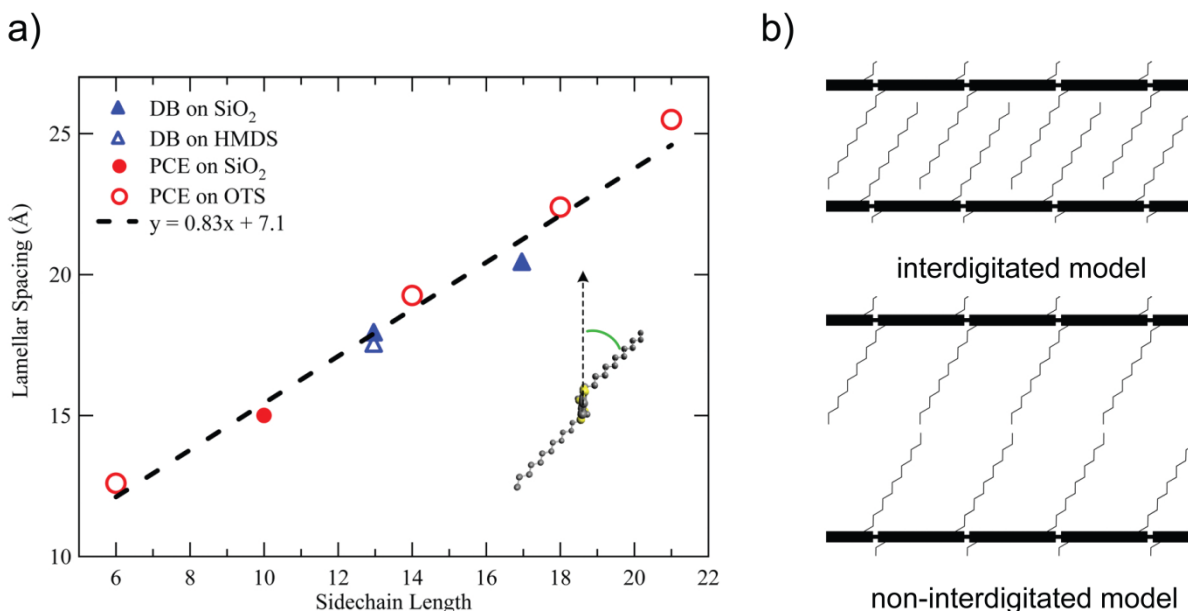


Fig. S2 (a) Lamellar spacing for various side-chain length variations of P2TDC_{xx}FT4 polymer films after 150°C thermal annealing. The solid triangles represent polymer thin films deposited from 1,2-dichlorobenzene (DB) on SiO₂ and open triangle represents films deposited on hexamethyldisilazane (HMDS) treated SiO₂.² The solid circles represent polymer thin films deposited from pentachloroethane (PCE) on SiO₂ and open circles represent films deposited on octyltrichlorosilane (OTS) treated SiO₂.³ Linear extrapolation shows backbone and uninterdigitated space contribution of 7.1 Å. These solvents and substrate treatments appear to have little influence on the lamellar spacing. (b) Side-chain models utilized to calculate the alkyl side-chain tilts.

The degree of interdigitation and the tilt of alkyl side-chains in the polythienothiophene thin films gives an indication to the polythienothiophene packing efficiency. Typically, the tilt and interdigitation can be measured by polarized IR and near-edge X-ray fine-structure spectroscopy, but these techniques were not available in our studies. In order to study the side-chain packing of the lamellar structure, the lamellar stacking distance is compared for various side-chain length tetrathienoacenes (Fig. S2) as reported

previously in literature or synthesized for this work. The linear trend of lamellar stacking distances has a slope of 0.83 \AA per carbon with a y-intercept of 7.1 \AA . The large y-intercept accounts for the space taken up by the thienothiophene backbone ($\approx 4 \text{ \AA}$) and the void or the uninterdigitated region between the alkyl side-chains ($\approx 3 \text{ \AA}$). The thienothiophene backbone in this family of polymer has been observed to take on a highly edge-on orientation,⁴ which is in agreement with our model. This linear trend of the lamellar stacking distances can be modeled with either interdigitated or non-interdigitated models⁵ (See Fig. S3).

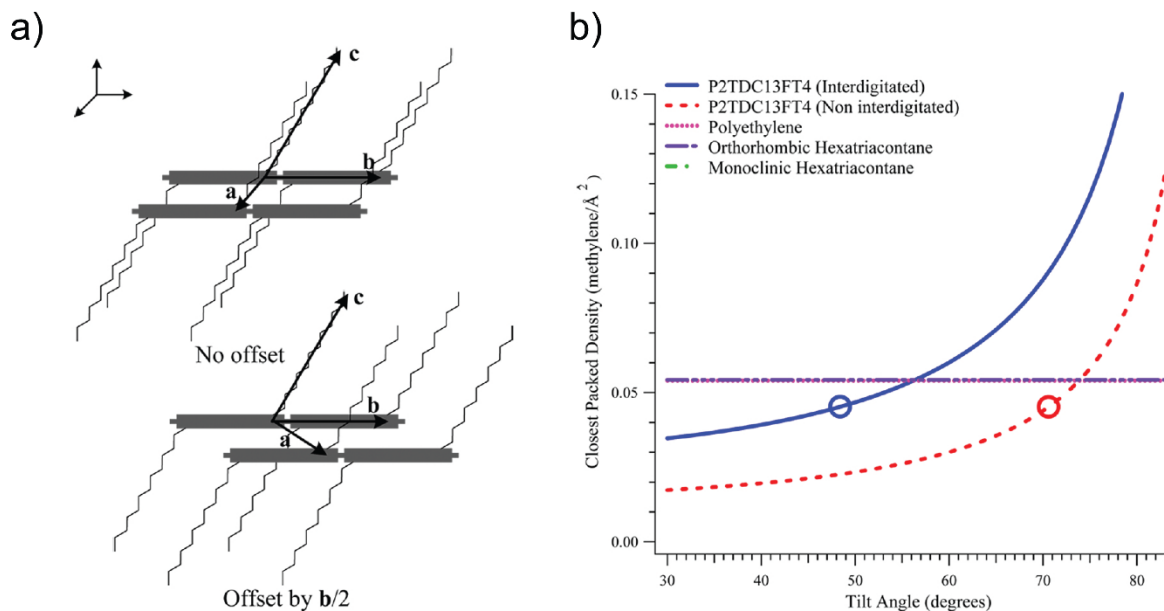


Fig. S3 (a) Models utilized to calculate the alkyl side-chain close packing area. (b) Side-chain packing density for various tilt angles for P2TDC13FT4 with and without interdigitation. The packing density of hexatriacontane and the predicted density of the C13 alkyl chain are shown for determination of the preferred angle. Circles denote the calculated tilts from the interdigitated and the non-interdigitated lamellar stacking distance models.

In the case of the interdigitated model, each carbon in the alkyl side-chain increases the lamellar spacing by $d_{c-c}\cos(\theta)$, where d_{c-c} is the carbon-carbon distance along the alkyl chain and θ is the side-chain tilt angle. For the non-interdigitated model, each carbon in the alkyl side-chain increases the lamellar spacing by $2d_{c-c}\cos(\theta)$, because of the end to end orientation of the alkyl side-chains. In both of these models, we make no assumptions about the exact orientation of the alkyl side-chain to the polymer backbone, meaning that alkyl chains are not necessarily in the same plane as the backbone, which is most likely the case based on the tilt angles calculated. Using the slope of 0.83 \AA and the unit length of the alkyl chain per carbon of 1.25 \AA , the alkyl chain tilt can be calculated to be 48.4° for the interdigitated

model and 70.6° for the non-interdigitated model. A tilt angle of $\approx 70^\circ$ is extreme and would lead to significant steric hindrance in the lamellae. Therefore, we rule out the possibility of a non-interdigitated model and conclude that in our system the side-chains are nearly completely interdigitated.

Additionally, a geometric analysis of the side-chain packing inspired by Kline et al.⁶ has been carried out to analyze the feasibility of interdigitation and to verify agreement with the previous analysis. Studies of paraffins, self-assembled monolayers of alkanethiols, and other polythiophenes have demonstrated that the area density of alkane side-chains has to be approximately 5.4×10^{-2} methylene/ \AA^2 to balance the van der Waals forces between the alkyl chains.^{6, 7}

The area of the side-chain close packing plane can be found by using the equation below, which is illustrated in Fig. S3.

$$Area = \left\| \left(\vec{a} - \frac{\vec{a} \cdot \vec{c}}{\|\vec{c}\|} \vec{c} \right) \times \left(\vec{b} - \frac{\vec{b} \cdot \vec{c}}{\|\vec{c}\|} \vec{c} \right) \right\|$$

In our model, \vec{a} points to the alkyl side-chain on the neighboring backbone, separated by the π - π stacking distance, \vec{b} points to the alkyl side-chain on the neighboring monomer, separated by the rigid backbone, and \vec{c} points along the alkyl side-chain. The alkyl side-chain is allowed to have a rotation in the $\vec{a} - \vec{b}$ plane and has a tilt angle of θ . In addition, we calculated two other possible scenarios of backbone packing: no offset between π - π stacked monomers and maximum offset of $\vec{b}/2$ (Fig. S3). In all of the cases, the area of the close packing plane simplifies to:

$$Area = d_{\pi-\pi} b \cos(\theta)$$

where $d_{\pi-\pi}$ is the π - π stacking distance and b is the backbone length. This demonstrates that there is no dependence on the tilt of the alkyl side-chain in the $\vec{a} - \vec{b}$ plane or on the relative offset between π - π stacked monomers. The methylene density can now be calculated by accounting for one carbon unit in the close packing area, as would be the case for non-interdigitated side-chains, or two units for interdigitated side-chains. Using this result with a π - π stacking distance of 3.84 \AA and backbone length of 17.3 \AA , the closest-packed density can be calculated for P2TDC13FT4 from the interdigitated and non-interdigitated models (see Fig. S3). The calculated packing densities for P2TDC13FT4 can be compared to the densities in monoclinic hexatriacontane⁸ ($\text{C}_{36}\text{H}_{74}$), with very well studied structure, or to the expected density based on the empirical formula⁷ for the cross-section of paraffin with 13 carbons in the chain. Our geometric model predicts a preferred side-chain tilt angle of 54° for the interdigitated model

and 73° for the non-interdigitated model. The tilt angles predicted by this model are in good agreement with the tilt values previously calculated based on lamellar spacing, represented by the open circles in Fig. S3. Once again, the large tilt angles in the non-interdigitated model rule out this possibility and thus support the nearly complete interdigitation of alkyl side-chains in tetrathienoacenes with agreement between the calculated preferred angle and the extrapolated tilt from the interdigitated model based on experimental data.

References

- 1 M. He and F. Zhang, *J. of Org. Chem.*, 2007, **72**, 442–451.
- 2 H. H. Fong, V. A. Pozdin, A. Amassian, G. G. Malliaras, D.-M. Smilgies, M. He, S. Gasper, F. Zhang and M. Sorensen, *J. of Am. Chem. Soc.*, 2008, **130**, 13202–13203.
- 3 M. He, J. Li, M. L. Sorensen, F. Zhang, R. R. Hancock, H. H. Fong, V. A. Pozdin, D.-M. Smilgies and G. G. Malliaras, *J. of Am. Chem. Soc.*, 2009, **131**, 11930–11938.
- 4 G. Giri, D. M. DeLongchamp, J. Reinspach, D. A. Fischer, L. J. Richter, J. Xu, S. Benight, A. Ayzner, M. He, L. Fang, G. Xue, M. F. Toney and Z. Bao, *Chem. Mater.*, 2015, **27**, 2350–2359.
- 5 T. Yamamoto, D. Komarudin, M. Arai, B. Lee, H. Suganuma, N. Asakawa, Y. Inoue, K. Kubota, S. Sasaki, T. Fukuda and H. Matsuda, *J. Am. Chem. Soc.*, 1998, **120**, 2047–2058.
- 6 R. J. Kline, D. M. DeLongchamp, D. A. Fischer, E. K. Lin, L. J. Richter, M. L. Chabinyc, M. F. Toney, M. Heeney and I. McCulloch, *Macromolecules*, 2007, **40**, 7960–7965.
- 7 V. Vand, *Acta Cryst.*, 1953, **6**, 797–798.
- 8 H. Shearer and V. Vand, *Acta Cryst.*, 1956, **9**, 379–384.